Available online at www.sciencedirect.com
ScienceDirect
Surface Science 601 (2007) 3350–3360
SURFACE SCIENCE
www.elsevier.com/locate/susc

The structure of the $V_2O_3(0001)$ surface: A scanned-energy mode photoelectron diffraction study

E.A. Kröger [a], D.I. Sayago [a,1], F. Allegretti [b,2], M.J. Knight [b], M. Polcik [a], W. Unterberger [a], T.J. Lerotholi [b], K.A. Hogan [c], C.L.A. Lamont [c], D.P. Woodruff [b,*]

[a] *Fritz-Haber-Institut der Max-Planck-Gesellschaft, Faradayweg 4-6, 14195 Berlin, Germany*
[b] *Physics Department, University of Warwick, Coventry CV4 7AL, UK*
[c] *Department of Chemical and Biological Sciences, University of Huddersfield, Queensgate, Huddersfield HD1 3DH, UK*

Received 30 April 2007; accepted for publication 5 June 2007
Available online 13 June 2007

Abstract

Scanned-energy mode photoelectron diffraction (PhD), using the O 1s and V 2p photoemission signals, together with multiple-scattering simulations, have been used to investigate the structure of the $V_2O_3(0001)$ surface. The results support a strongly-relaxed half-metal termination of the bulk, similar to that found in earlier studies of $Al_2O_3(0001)$ and $Cr_2O_3(0001)$ surfaces based on low energy electron and surface X-ray diffraction methods. However, the PhD investigation fails to provide definitive evidence for the presence or absence of surface vanadyl (V=O) species associated with atop O atoms on the surface layer of V atoms. Specifically, the best-fit structure does *not* include these vanadyl species, although an alternative model with similar relaxations but including vanadyl O atoms yields a reliability-factor within the variance of that of the best-fit structure.
© 2007 Elsevier B.V. All rights reserved.

Keywords: Surface relaxation; Surface structure; Vanadium oxide; Photoelectron diffraction

1. Introduction

Vanadium oxides play a major role in practical heterogeneous catalysis [1] and have, therefore, attracted significant attention in model surface science studies. In the case of vanadium sesquioxide, V_2O_3, interest in the bulk electronic and crystallographic properties has also been pursued due to the existence of a metal–insulator Mott transition that can be induced around room temperature by modest elevated pressures or slight doping by Cr or Ti (e.g. [2]). Like most oxides, a combination of factors including the difficulty of obtaining good single crystals, of finding a reliable and repeatable method of surface cleaning, and charging in the case of insulating crystals, means that almost all recent surface studies of V_2O_3 surfaces, invariably the (0001) surface, have been conducted on epitaxial thin films grown in situ in the UHV surface science chamber [3]. Well-ordered $V_2O_3(0001)$ films, as characterised by the low energy electron diffraction (LEED) pattern, have been grown on a range of substrates including W(110) [4], $Cu_3Au(100)$ [5], Au(111) [4], Pd(111) [6–10] and Rh(111) [11–13].

A key starting point in understanding the electronic and chemical properties of any surface is knowledge of the surface structure. However, quantitative experimental structural data on oxide surfaces is generally sparse, and in the case of $V_2O_3(0001)$ there appear to have been no such study by any method. Instead, the surface structure has been inferred from scanning tunnelling microscopy (STM) with atomic-scale resolution, and from theoretical total-energy calculations [14–17]. Clearly there is a need

* Corresponding author. Tel.: +44 2476 523378; fax: +44 2476 692016.
E-mail address: d.p.woodruff@warwick.ac.uk (D.P. Woodruff).
[1] Present address: Departamento de Física de la Materia Condensada, Universidad Autónoma de Madrid, 28049 Madrid, Spain.
[2] Present address: Karl-Franzens-Universität Graz, Institut für Physik, Bereich für Experimentalphysik, Universitätsplatz 5, 8010 Graz, Austria.

0039-6028/$ - see front matter © 2007 Elsevier B.V. All rights reserved.
doi:10.1016/j.susc.2007.06.014

for detailed experimental information on this structure. All that is known for certain experimentally (based on the LEED pattern and STM images reported in these existing publications) is that the surface of the as-prepared epitaxial films have a (1×1) surface mesh consistent with an absence of any surface reconstruction.

Two key questions relate to the structure of the $V_2O_3(0001)$ surface, namely the nature of the surface termination, and the magnitude of relaxations of the atomic positions in the near-surface region relative to the underlying bulk structure. At room temperature the bulk structure is trigonal (space group $R\bar{3}c$) and can be represented by a hexagonal unit cell with lattice parameters of $a = 14.00$ Å and $c = 4.95$ Å containing six V_2O_3 units [18]. Relative to the (0001) basal plane, the structure, as shown in Fig. 1, comprises alternate buckled layers containing 2 V atoms per unit mesh and planar layers containing 3 O atoms per unit mesh. The O layers are slightly laterally distorted relative to a true close-packing, and the nearest V atoms occupy three-fold coordinated sites relative to these O atom layers. Terminating the solid by a complete O layer, or a complete V buckled double-layer leaves a polar surface that is energetically unfavourable, so the preferred termination, supported by several total-energy calculations, is generally believed to be a 'half-metal' layer. Thus, if one regards the structure as comprising a layer structure of the form $\cdots$V′OVV′OV$\cdots$, where the VV′ terminology relates to the two buckled components of the V layers, the anticipated termination is $\cdots$OVV′OV. However, it is generally believed that the method of preparation of the epitaxial films, by evaporation of V in a partial pressure of oxygen gas, leads to a stable structure in which O atoms are adsorbed atop the V atoms of the terminating metal half-layer to produce surface vanadyl (V=O) species.

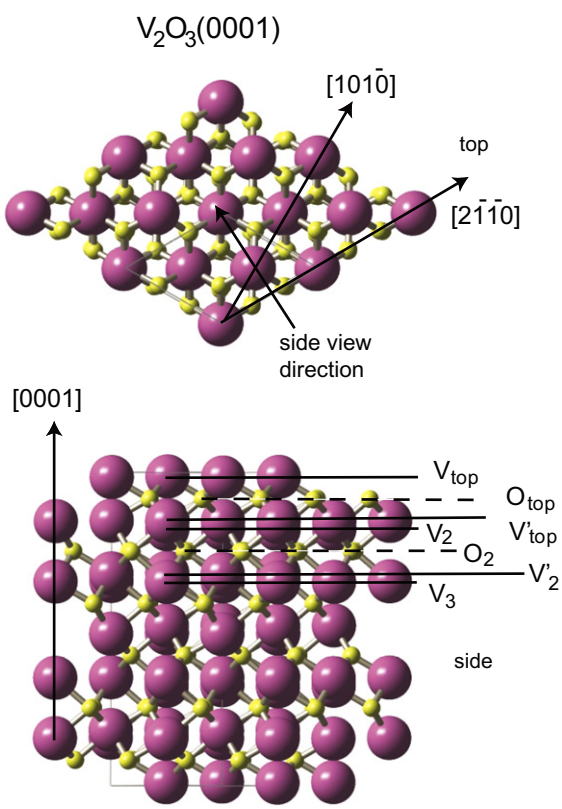

Fig. 1. Side and plan (along [0001]) views of a diagram of the V_2O_3 bulk structure. The labelling of the outermost few atomic layers (for a half-metal termination) define the convention used in the text and tables.

While the current understanding of the surface relaxations is based entirely on the theoretical total-energy calculations, there is some experimental evidence for the presence of the surface vanadyl species that are also favoured by these theoretical results. In particular, a vibrational mode seen in electron energy loss spectroscopy (EELS) at ~127–129 meV [4,13], also seen in reflection–absorption infrared spectroscopy (RAIRS) [4], is attributed to the V=O stretching frequency. Experiments believed to produce a chemical reduction of the surface, and a removal of the vanadyl O atoms, using incident electron irradiation [4], do indicate some attenuation of this absorption band, although it never seems to be lost entirely. Moreover, an alternative process of reaction with oxygen at 500 °C which leads to the formation of a $(\sqrt{3} \times \sqrt{3})R30°$ surface phase, believed to arise due to partial removal of the surface vanadyl species (as implied by STM images), does not lead to any detectable attenuation of the vanadyl-assigned EELS peak [13]. On the other hand, two other spectral features thought to be characteristic of the surface vanadyl, namely a weak shoulder on the V $2p_{3/2}$ peak seen in X-ray photoelectron spectroscopy (XPS), and a feature in the V 3d valence band photoemission, do appear to be influenced by these alternative methods of depleting the vanadyl surface coverage [4,13]. Interestingly, a low energy ion scattering spectroscopy (ISS) study of a $V_2O_3(0001)$ film grown on $Cu_3Au(100)$, combined with STM, concluded that the surface structure was a double-metal rather than single-metal termination, although with a fractional coverage of O atoms; interestingly, the possibility that these O atoms occupied atop sites, as in the expected vanadyl species, was specifically excluded [5].

While there are no quantitative experimental structural studies of the $V_2O_3(0001)$ surface, there have been some investigations of this type on the (0001) face of Al_2O_3 [19,20] and Cr_2O_3 [21,22] using quantitative LEED [20,21] and surface X-ray diffraction (XRD) [19,22]. All of these investigations find that the half-metal termination of the surface is favoured (although the XRD study of Cr_2O_3 found evidence of significant Cr occupation of interstitial subsurface sites), and that the outermost layer spacings are strongly contracted relative to the ideal bulk structure termination. An ion scattering study of the $Al_2O_3(0001)$ surface came to a similar conclusion [23]. Vibrational spectroscopy data have been interpreted in terms of the presence of a chromyl (Cr=O) surface species (with O atoms atop the Cr atoms of the surface metal half-layer) on the epitaxial thin films grown on Cr(110) [24], similar to the vanadyl species proposed to terminate as-grown films of V_2O_3. However, the LEED study of this surface does not appear

have considered the possible influence of the presence of such a species in the structure determination. Interestingly, the LEED study of Al_2O_3 [20] did include consideration of a structural model including atop O atoms such as might be associated with an Al=O surface species, although the motivation for studying this model was to explore the possible role of water adsorption; this structural model was not favoured by the analysis.

Here we present the results of a quantitative experimental investigation of the surface structure of as-prepared epitaxial $V_2O_3(0001)$ film grown on Pd(111) using the technique of scanned-energy mode photoelectron diffraction (PhD). Photoelectron diffraction [25,26] exploits the coherent interference between the directly-emitted component of a photoelectron wavefield emitted from a core level of an atom and the components of the same wavefield elastically scattered by the surrounding atoms. This interference provides information on the relative position of the emitter and scatterer atoms. This technique is especially well-suited to determining the location of adsorbed atoms and molecules on a surface, a situation in which the adsorbate emitter atoms can be determined relative to the underlying substrate atoms, exploiting the dominant role of backscattering in the PhD modulations. For clean surfaces, in the absence of a measurable shift in the photoelectron binding energy associated with emitter atoms in the surface layer, the technique is less incisive, but a recent application of this approach to the clean $TiO_2(110)(1\times1)$ surface has proved quite effective and led to optimised surface relaxation values in good agreement with recent studies by other, more traditional, methods [27]. As we shall show, the use of O 1s and V 2p PhD spectra can provide significant information on the structure of the $V_2O_3(0001)$ surface, providing clear evidence of strong modifications of the outermost layer spacings similar to those found for Al_2O_3 and $Cr_2O_3(0001)$ surfaces, although we find the results are inconclusive with respect to the possible structure, or even the presence, of surface vanadyl species.

2. Experimental and computational details

The experiments were conducted in an ultra-high vacuum surface science end-station equipped with typical facilities for sample cleaning, heating and cooling. This instrument was installed on the UE56/2-PGM1 beamline of BESSY II which comprises a 56 mm period undulator followed by a plane grating monochromator [28]. Different electron emission directions can be detected by rotating the sample about its surface normal (to change the azimuthal angle) and about a vertical axis (to change the polar angle). Sample characterisation *in situ* was achieved by LEED and by soft-X-ray photoelectron spectroscopy (SXPS) using the incident synchrotron radiation. Both the wide-scan SXPS spectra for surface characterisation, and the narrow-scan O 1s and Ti 2p spectra used in the PhD measurements, were obtained using an Omicron EA-125HR 125 mm mean radius hemispherical electrostatic analyser, equipped with seven-channeltron parallel detection, which was mounted at a fixed angle of 60° to the incident X-radiation in the same horizontal plane as that of the polarisation vector of the radiation.

The V_2O_3 (0001) films were grown on a Pd(111) substrate using methods initially characterised by the group of Netzer and coworkers [6,7,9]. The Pd(111) substrate was first cleaned *in situ* by cycles of 1 keV Ar^+ ion bombardment and annealing to 600 °C to achieve a clean (1×1) ordered surface as indicated by SXPS and LEED. The oxide films were then grown from a vanadium rod evaporator in an oxygen partial pressure of 2×10^{-7} mbar at a rate of 0.5 ML/min, based on a calibration (in UHV) of the V evaporation source using a Quartz Crystal Monitor with a typical total deposition time of ~30 min; 1 ML here corresponds to a complete V_2O_3 layer (i.e. one O layer and two V half-layers or one V′OV unit in the bulk layer structure) in $V_2O_3(0001)$. The Pd(111) substrate was held at ~300 °C throughout the dosing. After the evaporator was switched off the sample was cooled in stages to ~150 °C with the oxygen partial pressure retained. After then pumping out the oxygen to restore UHV the sample was heated for 1–2 min to ~400 °C to improve the surface ordering. Higher annealing temperatures were not used after preliminary studies revealed that Pd diffusion occurred into the film from the substrate at temperatures of ~450 °C or higher. The resulting $V_2O_3(0001)$ films with an estimated thickness of 30–50 Å showed the expected stoichiometry and order as judged by SXPS and LEED. The Pd 3p photoemission signal was completely suppressed by this film, an important requirement for the O 1s PhD spectra collection due to the closely similar binding energies of these states. Note that, relative to the Pd(111) clean surface, the resulting LEED pattern has $(\sqrt{3}\times\sqrt{3})R30°$ periodicity, consistent with a (1×1) termination of $V_2O_3(0001)$. The LEED pattern showed 6-fold rotational symmetry, consistent with the expected presence of two possible surface terminations (whatever elemental termination is involved), related by a 180° rotation, that are a characteristic of the corundum structure.

Fig. 2 shows a typical SXPS spectrum in the energy range of the V 2p and O 1s photoemission peaks from an as-prepared $V_2O_3(0001)$ film, recorded at a polar emission angle of 60° leading to some enhancement in the surface specificity. As has been remarked by previous authors [29,4], the spectral widths of the V 2p peaks from V_2O_3 are significantly larger than those typically seen from V_2O_5. Early discussions of the origin of this effect centred on electronic many-body effects in the valence electrons or multiplet splitting [30], but more recent papers have suggested it is due to the presence of at least two chemically-shifted components; in particular, a component at lower kinetic energy (higher binding energy) by ~2.0 eV has been attributed to emission from surface V atoms, and specifically to those in vanadyl V=O groups [4,12]. The fact that this component appears relatively more intense at grazing emission angles supports the idea that this is a surface-specific signal. We may note,

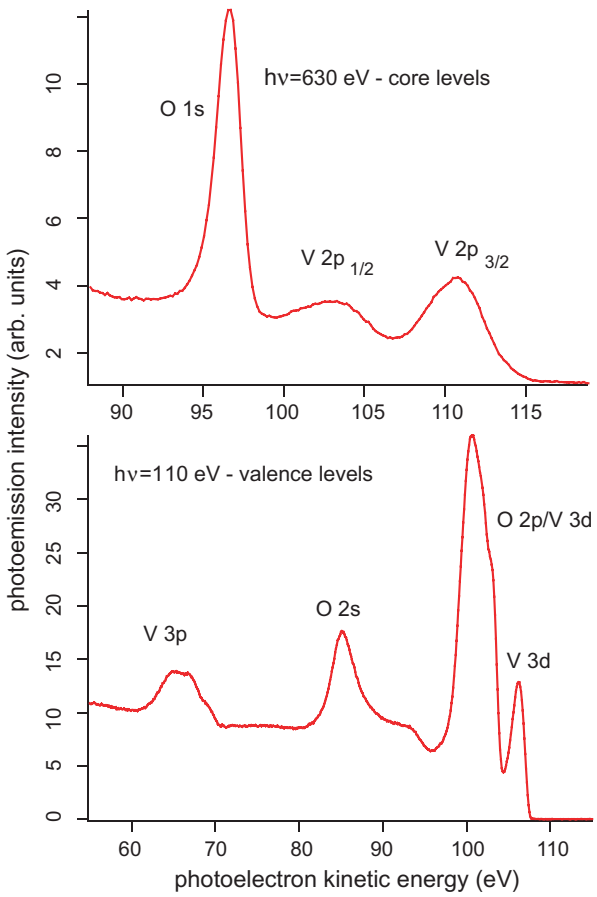

Fig. 2. Typical SXPS spectrum, in the range of the V 2p and O 1s emission peaks, and of the V 3p, O 2s and O 2p/V 3d valence band peaks, recorded from the as-prepared surface of a $V_2O_3(0001)$ epitaxial film grown on Pd(111) at a polar emission angle of 60°.

however, that the V 3p photoemission spectrum recorded from V_2O_3 shows three distinct components (Fig. 2), and at least some of this complexity seems likely to have its origins in multiplet splitting, which is expected to be significantly more important for the 3p emission [30].

Scanned-energy mode photoelectron diffraction involves the measurement of the photoemission intensity from a core level in specific directions as a function of the photoelectron energy. Modulations in the resulting spectrum arise from the change in phase of directly-emitted and scattered components of the photoelectron wavefield as the photoelectron wavelength changes, and can be interpreted in terms of the scattering path lengths and thus the local geometry. In the present case the PhD modulation spectra were obtained by recording a sequence of photoelectron energy distribution curves (EDCs) around the O 1s and V $2p_{3/2}$ peak at 4 eV steps in photon energy in the photoelectron kinetic energy range of approximately 70–320 eV for each of a number of different emission directions in the polar emission angle range from 0° (normal emission) to 60° in the two principle azimuthal planes, $[2\bar{1}\bar{1}0]$ and $[10\bar{1}0]$ (labelled in Fig. 1). Each of these data sets was processed following our general PhD methodology (e.g. [25]) in which the individual EDCs are fitted by the sum of Gaussian peaks, associated steps and a template background extracted from the high kinetic energy tails of the individual EDCs.

In the case of the V $2p_{3/2}$ emission, attempts were made to achieve a reliable separation into the two chemically-shifted components described above. If one component really is due to vanadyl vanadium atoms on the surface, the PhD spectra of this component should provide significantly greater surface specificity in the structural analysis. However, no reliable separation of the components proved possible, so this signal was represented by a single (broad) Gaussian peak. We should note that previous separations of the two components have been performed on (individual) spectra measured at grazing emission angles, leading to a significant enhancement in the relative intensity of the surface component. In our PhD data, the emission angles were chosen to optimise the photoelectron diffraction effects, rather than to enhance the surface specificity. Thus, it is clear that in the V 2p spectrum shown in Fig. 2, at a polar emission angle of 60° and a kinetic energy of ~100 eV, a reasonable separation of the main peaks and the low kinetic energy shoulder ought be achievable. Most of the PhD data that yielded reasonable diffraction modulations, however, were recorded near normal emission, with substantially reduced surface specificity. Moreover, the PhD data include measurements up to kinetic energies of ~300 eV, at which both the monochromator and electron spectrometer resolution is inferior, and the surface specificity is further reduced. It is certainly possible that individual spectra recorded at normal emission and higher kinetic energy, but using higher instrumental resolution and very much longer (at least 10×) data collection times, might allow the peak separation to be achieved, but the total collection times for the many spectra needed to record a PhD modulation spectrum in even a single emission geometry would become prohibitive.

The intensity of the O 1s and V $2p_{3/2}$ peaks extracted in this way were then plotted as a function of kinetic energy, $I(E)$. The shape of $I(E)$ contains not only the PhD modulations, but longer period variations due to the transmission functions of the monochromator and the analyser, as well as the variation in the atomic photoionisation cross-section. These effects are approximated by fitting a spline, $I_0(E)$, through $I(E)$. The PhD modulation function, $\chi(E)$, is then given by

$$\chi(E) = \frac{I(E) - I_0(E)}{I_0(E)}$$

These PhD modulation spectra form the basis of the structure determination. The method of achieving this is based on multiple-scattering simulations for trial model structures which are compared with the experimental modulation spectra. These calculations were performed with computer codes developed by Fritzsche [31–33] that are based on the expansion of the final state wave-function into a sum over all scattering pathways which the electron can

take from the emitter atom to the detector outside the sample. Key features are the treatment of double and higher order scattering events by means of the Reduced Angular Momentum Expansion (RAME) and inclusion of the effects of finite energy resolution and angular acceptance of the electron energy analyser analytically. Anisotropic vibrations for the emitter atom and isotropic vibrations for the scattering atoms are also taken into account. The quality of agreement between the theoretical and experimental modulation amplitudes is quantified by the use of an objective reliability-factor (R-factor) defined [25,26] such that a value of 0 corresponds to perfect agreement and a value of 1 to uncorrelated data. Note that our general methodology is to calculate the R-factor from the complete set of experimental PhD spectra used in the theory/experiment comparison. In addition to this value of R_{global}, however, one can calculate R-factors for individual PhD spectra recorded for a particular emitter in a particular geometry, and in the present analysis we will stress the utility of one such parameter.

Because our experimental O 1s and V $2p_{3/2}$ PhD data do not distinguish between O and V atom emitters in the surface and the bulk, the calculations were performed by summing (incoherently) the results of calculations conducted for emitter atoms in several outermost near-surface layers. The attenuation of the signal from subsurface layers due to inelastic scattering, combined with multiple elastic scattering, included in the multiple-scattering simulations, ensures that a relatively small number of layers contribute to this summation. In the present case it was found that summing over 4 layers (each layer comprising one O layer and two V half-layers – i.e. one V′OV slab) was sufficient to achieve reasonable convergence and a consistent description of the resulting PhD spectra.

3. PhD results and multiple-scattering calculations

The overall objective of the structural analysis for $V_2O_3(0001)$ was aimed at answering two questions, namely, what is the correct model of the surface termination, and what is the detailed geometry of the outermost layers? In principle, at least, one may imagine three basically distinct terminations, an oxygen termination (···V′OVV′O), a double-metal termination (···V′OVV′) or a single-metal or half-metal termination (···V′OVV′OV). In addition, the half-metal termination may have adsorbed O atoms atop the outermost (half-metal) V atoms to produce surface vanadyl species (···V′OVV′OV=O). For each of these terminations one may expect different relaxations, mainly perpendicular to the surface, of the outermost layer spacings. There is therefore quite a large parameter space of structures to be investigated, based on the different termination models with several interlayer spacing parameters to be optimised for each model. The fact that calculations had to be performed for each structurally-distinct emitter atom in the outermost four layers (corresponding to 12 O emitters and 8 V emitters for a half-termination model) compounds the computational demands. To ameliorate this problem, however, we note that there exist specific structural models for each termination (with associated structural parameter values) derived from density functional theory (DFT) total-energy calculations by Czekaj, Hermann and Witko [14–16] and of Kresse et al. [17] based on clusters and slabs, respectively. We have therefore first conducted PhD calculations for the two principal, energetically favoured, half-metal and half-metal-plus-vanadyl energetically-optimised structures, together with idealised starting structures based on ideal bulk-termination models in which all interlayer spacings are identical to those of the bulk solid. Also included in the initial tests was the energetically-optimised double-metal-termination model.

As an example of these results, Fig. 3 shows a comparison of the experimental PhD spectra with the results of multiple-scattering calculations for the model showing the lowest R-factor values (see Table 1) corresponding to a half-metal bulk termination with added vanadyl O atoms (···V′OV=O), using the interlayer spacings found in the DFT calculations of Czekaj et al. The experimental data set used for this model, and all other models considered here, comprises four O 1s and three V $2p_{3/2}$ PhD spectra. These spectra were chosen from an original larger set of fifteen spectra, eight O 1s and seven V $2p_{3/2}$, in order to allow the full structural optimisation calculations to be completed in a realistic time-scale. In selecting this subset of spectra we note that a characteristic feature of most of the experimental spectra from this surface is very weak modulations, in many cases less than ±10%. In PhD studies from adsorbate atoms occupying single high-symmetry sites and measured in near-neighbour backscattering directions, we have commonly observed modulation amplitudes

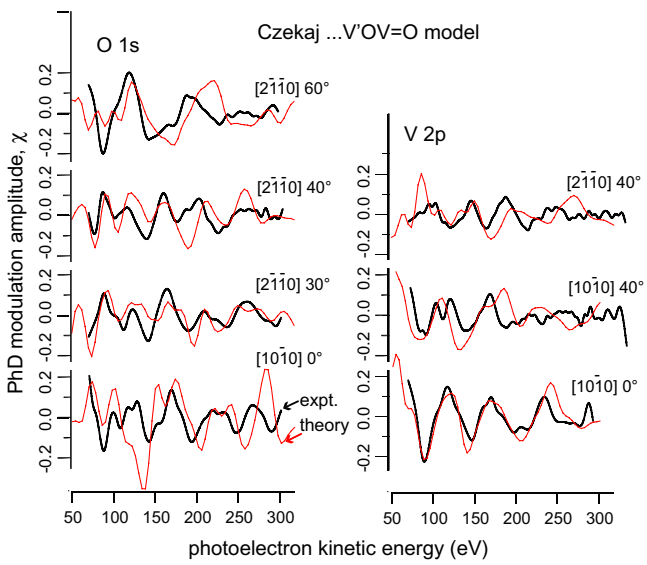

Fig. 3. Comparison of the set of experimental O 1s and V 2p PhD spectra used in this investigation of the $V_2O_3(0001)$ surface with the results of multiple-scattering calculations for the vanadyl-covered half-metal termination based on the exact structural parameter values given by total-energy calculations by Czekaj et al.

Table 1
Summary of the initial structural models of $V_2O_3(0001)$ tested and the R-factors found in comparison with the experimental PhD modulation spectra

Model	...V′OV half-metal				···V′OV half-metal + vanadyl=O				Double-metal ···V′OVV′
Model/ parameter	Bulk	Czekaj	Kresse	Czekaj vanadyl minus=O	Bulk plus=O	Czekaj	Kresse	Czekaj ···V′OV +=O	Czekaj
R_{global}	0.69	0.66	0.77	0.63	0.70	0.63	0.68	0.72	0.67
R_{V2pNE}	0.34	0.76	0.85	0.43	0.23	0.19	0.28	0.24	0.37
V_{top}–V′ (Å)	–	–	–		–	–	–	–	0.52
V_{top}–=O (Å)	–	–	–	–	1.61	1.59	1.61	1.61	–
O_{top}–V_{top} (Å)	0.98	0.68	0.35	0.82	0.98	0.82	0.75	0.68	0.59
V'_{top}–O_{top} (Å)	0.98	0.98	1.12	0.93	0.98	0.93	0.99	0.97	1.09
V_2–V'_{top} (Å)	0.36	0.27	0.22	0.34	0.36	0.34	0.28	0.27	0.18
O_2–V_2 (Å)	0.98	0.96	1.13	0.96	0.98	0.96	1.08	0.96	0.98
V'_2–O_2 (Å)	0.98	0.98	1.01	0.98	0.98	0.98	0.99	0.98	0.98
V_3–V'_2 (Å)	0.36	0.36	0.38	0.36	0.36	0.36	0.41	0.36	0.36
O_3–V_3 (Å)	0.98	0.98	1.01	0.98	0.98	0.98	1.00	0.98	0.98

Apart from the 'ideal' bulk-termination model, the interlayer spacings are based on those given in the total-energy calculations presented by Czekaj et al. [16] and Kresse et al. [17].

of ±40% or more, and in these cases both the experimental data and the theoretical calculations can be expected to be at their most reliable. In these situations low R-factors (generally ~0.20 or less) are found for the best-fit structural models. For adsorbate atoms in low symmetry sites, weaker modulations (~±20%) are generally seen due to the effect of averaging over symmetrically-equivalent domains, and the resulting best-fit R-factors are larger (~0.30–0.40). The present system, involving emitters in multiple layers with distinct local geometries, is therefore one in which weak modulations may be expected, and this necessarily lowers the reliability of the data and the calculations, despite considerable care to establish reproducibility in the main experimental modulations measured from several different surface preparations. Much higher minimal R-factors are therefore to be expected. Nevertheless, the most important criterion used to select the optimal subset of PhD spectra was the sensitivity of the simulations to the structural model. All of the spectra excluded from the final optimisation showed very weak variations in the single-spectrum R-factor between different structural models.

Fig. 3 clearly shows that the general level of agreement between theory and experiment for the energetically-optimised vanadyl-terminated structure is no better than modest, a subjective judgement supported by the rather high global R-factor value of 0.63. Table 1 shows the structural parameter values used in the full range of initial test structures. Four different sets of parameter values were used for the basic half-metal-termination model (···V′OV), namely the ideal bulk termination, the minimum-energy structures as determined by the two sets of DFT calculations (labelled Czekaj and Kresse), and in addition the Czekaj et al. minimum-energy structure determined for vanadyl termination (···V′OV=O), but with the vanadyl O atoms removed. Similarly, four alternative sets of interlayer spacings were used for the vanadyl-terminated surface model, two from the DFT calculations for this structure, together with two others generated by simply adding a vanadyl O atom to two of the half-metal termination structures. Both sets of theoretical total-energy calculations find the vanadyl termination to have the lower energy, while general electrostatic energy considerations favour a half-metal termination (as found for Al_2O_3 and Cr_2O_3 (0001) surfaces) over any other simple bulk termination, so these two basic models are the ones favoured in all existing literature. As an additional model a DFT-optimised double-metal termination was also considered. Evidently none of these models and associated interlayer spacings give a very good description of the PhD data; as shown in Table 1, all these structures give high R_{global} values in the range 0.63–0.77.

In addition to R_{global}, Table 1 shows the values of the R-factor obtained for just one of the PhD spectra, namely that recorded at normal emission from the V $2p_{3/2}$ photoemission peak. As is shown in Fig. 3, this experimental PhD spectrum is the one that shows the strongest modulations, apparently dominated by a single period, and as such is the spectrum we might expect to be best reproduced by multiple-scattering calculations for the correct structural model. This judgement is also reflected in the associated R-factor values, which not only show a much larger spread for the different structures (0.19–0.85), but also have a lowest value in the range to be expected for a good fit. This large variation in the quality of the fits is also seen in the visual comparison of the theoretical calculations and this experimental PhD spectrum shown in Fig. 4. We have therefore used this single-spectrum R-factor as an additional criterion in distinguishing the structural models. This criterion rather clearly favours the group of test structures involving the vanadyl half-metal termination, with the interlayer spacings calculated by Czekaj et al. giving rather good agreement for this one spectrum, as reflected in the single-spectrum R-factor of 0.19, and also in visual inspection of Fig. 3.

Of course, so far we have only compared the results for constrained structural models in which all interlayer spacings were fixed on the basis of a simple guess (bulk

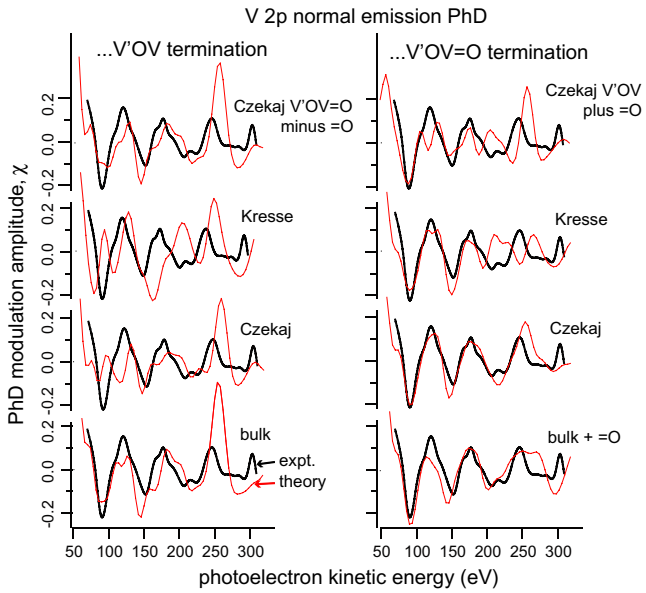

Fig. 4. Comparison of the experimental V 2p normal emission PhD spectrum with the results of multiple-scattering calculations for the half-metal and half-metal-plus-vanadyl oxygen terminations of $V_2O_3(0001)$ using the different sets of interlayer spacings as listed in Table 1.

termination) or using the results of previous DFT calculations. We may expect to find significantly better fits to the PhD spectra by a structural optimisation, adjusting each of the structural parameter values. To achieve this we made use of the automated search procedure based on a Newton–Gauss algorithm that is built into the Fritzsche multiple-scattering codes. In searching in a multi-parameter space it is important, of course, to ensure that one locates the global minimum, and for this reason it is helpful to start the optimisations from different sets of initial parameter values. In addition, the results of Table 1 do not provide a clear basis for distinguishing the two half-metal-termination models involving the presence or absence of vanadyl O atoms, so both models have been optimised. In each case two sets of starting values of the interlayer parameter values were used, those of the ideal bulk termination (with and without an added vanadyl O atom), and those of the DFT-optimised vanadyl-terminated surface given by Czekaj et al. (with and without the vanadyl O atom).

The results of these optimisations are summarised in Table 2. In the case of the two vanadyl-covered starting models, the final optimised structures are essentially identical, with differences in interlayer spacings in almost all cases of no more than 0.02 Å, and differences in the *R*-factors of 0.01. These optimisations thus clearly define a single well-defined solution. For the two non-vanadyl half-metal termination structural optimisations, however, one starting structure converged on a solution with substantially lower *R*-factor values that the other. Starting from the DFT (Czekaj et al.) optimised vanadyl-terminated model (the one giving the best agreement of the un-optimised structures see Table 1), but with the vanadyl O atom removed,

Table 2
Summary of the parameter values for the optimised structural models of $V_2O_3(0001)$ based on different starting structures, and their *R*-factors found in comparison with the experimental PhD modulation spectra

Model	···V′OV half-metal		···V′OV half-metal + vanadyl=O	
Starting model/ parameter	Bulk	Czekaj vanadyl minus=O	Bulk plus=O	Czekaj
R_{global}	0.55	0.46	0.52	0.53
R_{V2pNE}	0.39	0.20	0.23	0.24
V_{top}–=O (Å)	–	–	1.54	1.55
O_{top}–V_{top} (Å)	0.98	0.68	0.69	0.69
V'_{top}–O_{top} (Å)	0.92	0.93	1.03	1.05
V_2–V'_{top} (Å)	0.39	0.35	0.32	0.34
O_2–V_2 (Å)	1.02	1.02	1.07	0.95
V'_2–O_2 (Å)	0.98	0.98	0.98	0.98
V_3–V'_2 (Å)	0.36	0.36	0.36	0.36
O_3–V_3 (Å)	0.98	0.98	0.98	0.98

leads to the lowest overall *R*-factor values of all of these optimisations ($R_{global} = 0.46$, $R_{V2pNE} = 0.20$), but starting from bulk values of the interlayer spacings led to much higher *R* values (0.55 and 0.39 respectively). Inspection of the interlayer spacings indicates that the key difference is that the outermost V–O (O_{top}–V_{top}) interlayer spacing in this inferior solution has remained at the bulk value and failed to contract in the same way as all the other solutions. We infer that the optimisation procedure in this case has failed to get out of a local minimum in structural parameter space, as this is clearly not the global minimum. A comparison of the experimental and theoretical PhD spectra for the best-fit (non-vanadyl) half-metal-termination model of Table 2 is shown in Fig. 5. While the agreement is still

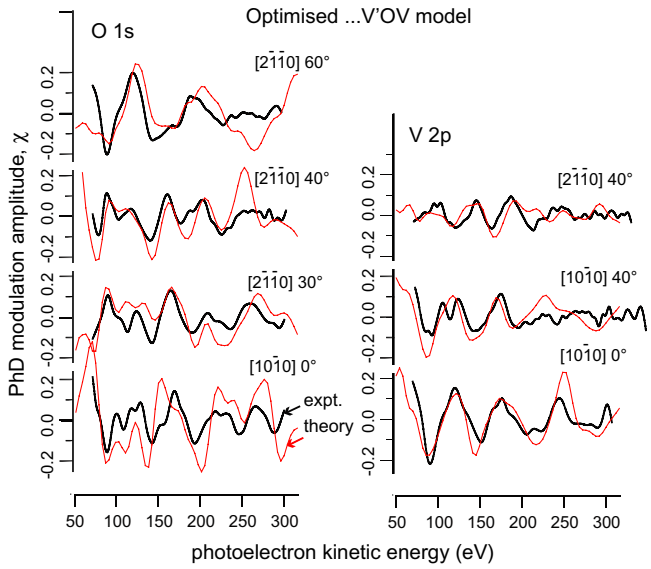

Fig. 5. Comparison of the set of experimental O 1s and V 2p PhD spectra used in this investigation of the $V_2O_3(0001)$ surface with the results of multiple-scattering calculations for the optimised non-vanadyl half-metal termination structure corresponding to the lowest values of the *R*-factors in Table 2.

far from perfect, the theoretical spectra do reproduce all the main features of the experimental data quite well.

A striking feature of the results of Table 2 is that while the initial tests without structural optimisation (Table 1), found the vanadyl-covered half-metal termination to be consistently preferred, full optimisation finds lower R-factor values for the half-metal termination *without* the surface vanadyl O atoms. Is this difference significant, and what is the precision of the interlayer spacings? To answer these questions we use an approach based on that of Pendry which was derived for LEED [34]. This involves defining a variance in the minimum of the R-factor, $R_{\min}$, $\mathrm{var}(R_{\min}) = \sqrt{(2/N)} \cdot R_{\min}$ where N is the number of independent pieces of structural information contained in the data. The detailed way N is calculated is specific to the multiple-scattering codes used in our analysis, and is described in more detail elsewhere [35]. All structural models and parameter values giving structures with R-factors less than $R_{\min} + \mathrm{var}(R_{\min})$ are regarded as falling within one standard deviation of the 'best fit' structure.

In general these criteria have been applied to R_{global}, but recognising that specific PhD spectra (recorded from a particular emitter in a favoured direction) can show particularly strong sensitivity to one or more structural parameters, it is also relevant to consider the effect of applying similar criteria to individual spectral R-factors. Of course, the data range in such a spectrum is smaller than in the complete data set, so even if the associated $R_{\min}$ is smaller, the associated variance may not be. As shown in Table 2, the lowest R-factor values ($R_{\mathrm{global}} = 0.46$, $R_{\mathrm{V2pNE}} = 0.20$) correspond to the non-vanadyl termination, and the associated variances of these two R-factors are found to both have the value of 0.10, the lower $R_{\min}$ of the single V 2p spectrum being offset by effect of the smaller data range. The corresponding R-factors for the best-fit vanadyl termination structure ($R_{\mathrm{global}} = 0.52$, $R_{\mathrm{V2pNE}} = 0.23$) therefore both fall within the variance, and no formal distinction can be drawn between the two structures. The inability to reach a clear conclusion regarding the presence or absence of the surface vanadyl oxygen on the basis of the PhD data is disappointing, but perhaps not entirely surprising. In particular, this structural model contains only one vanadyl O atom per surface unit mesh, whereas the underlying bulk contains three O emitter atoms in each layer. With a significant contribution to the measured O PhD modulations from 4 layers (12 O atoms per unit mesh), the vanadyl O emitters contribute only modestly to the total O 1s signal, while their weak forward scattering of V 2p photoelectrons will have little effect on the V 2p PhD spectra, one of which proves particularly sensitive to other structural parameters.

In order to estimate the precision of the interlayer spacing values given in Table 2, calculations were performed in which each layer of atoms was displaced perpendicular to the surface until the R-factor values fell outside the variance, in all cases keeping all other atoms fixed. This provides a measure of the precision of location of each atomic layer. Strictly, of course, the interlayer spacings involve the effects of imprecise knowledge of the exact location of two layers, but the correct way to combine these errors is not clear. The usual addition of errors in quadrature assumes the errors to be uncorrelated, but this is not the case. For example, displacing emitter atoms in layer n (where n increases as one moves below the surface) means that the interlayer spacing of this atom is changed relative to all the underlying atoms, so the precision in this parameter determined in this way is probably better that the true precision in the interlayer spacing between layers n and $n+1$. However, moving atoms in layer $n+1$ alone also changes the interlayer spacing between layers n and $n+1$, so adding the two errors in quadrature would count some sources of error twice, and thus underestimate the precision. It is probably most appropriate, therefore, to regard the larger of the errors in the location of the individual layers as indicative of the precision of the interlayer spacing. These error estimates are shown separately in Table 3. As we have already noted, the V 2p normal emission spectrum (with a very low R-factor for some structures) proves very sensitive to some individual structural parameter values, and in these cases this R-factor exceeds the variance even when R_{global} lies within the variance. The error estimates given in Table 3 correspond to those associated with the more sensitive R-factor of each parameter.

Table 3
Precision estimates for the location of the near-surface layers of $V_2O_3(0001)$ in the optimised structural model obtained from the PhD analysis

Layer	Error estimate (Å)
V_{top}	−0.20/+0.10
O_{top}	−0.10/+0.15
V'_{top}	−0.05/+0.10
V_2	−0.25/+0.10
O_2	−0.10/−0.15

4. General discussion and conclusions

Fig. 6 provides a graphical representation of the interlayer spacings found for the two alternative best-fit structural models obtained in this PhD analysis with the comparable values obtained by the total-energy calculations, and also for the bulk half-metal termination. The information is the same as that reported in Table 2, but the graphical representation allows a simpler visual comparison. The data are shown in two modes. In the upper half of the figure the deepest subsurface (bulk) layers in the different models are aligned, thus providing an indication of the relaxations relative to the underlying bulk, the most usual way of describing such structures. In the lower half of Fig. 6 the outermost half-metal layers are aligned. This representation more properly reflects the structure as determined by PhD, because this technique determines the location of near-subsurface layers relative to the emitter atoms in the surface layers.

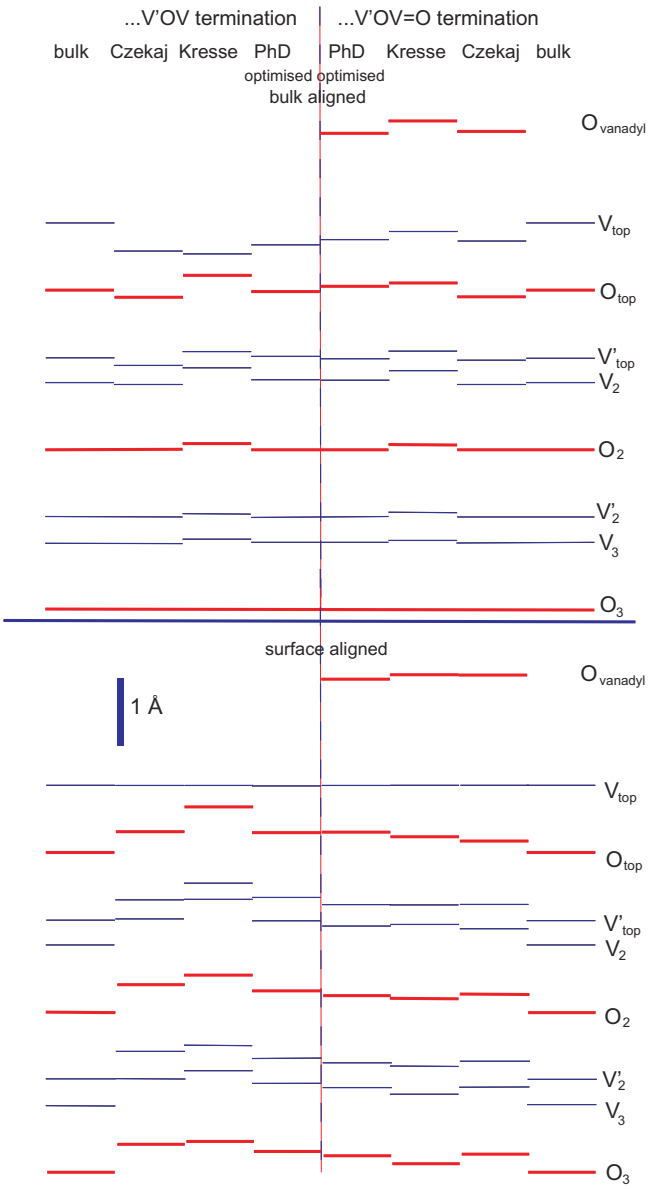

Fig. 6. Geometrical representation of the interlayer spacings of $V_2O_3(0001)$ for the two PhD optimised structures (with and without surface vanadyl species) compared with the DFT-optimised structures of Czekaj et al. and Kresse et al., and with the bulk structure. In the upper part of the diagram the lowest (O_3) layer is aligned in the different models, while in the lower part the outermost V_{top} layer is aligned. The 1 Å vertical bar provides a basis for understanding the significance of the estimated precision in layer spacings of ~0.05–0.25 Å as listed in Table 3.

One thing that is immediately clear from Fig. 6 is the substantial contraction of the spacing of the outermost V atoms (V_{top}) relative to the underlying bulk when compared to the bulk-termination model. This effect is reproduced by the total-energy calculations for both the vanadyl and non-vanadyl half-metal-termination models. Comparison of these relaxations with the values predicted theoretically for the two alternative terminations does not, therefore, provide an indirect means of distinguishing the preferred termination on the basis of our PhD structural solutions. What is clear from Fig. 6, however, is that the outermost V–O interlayer spacing (V_{top}–O_{top}), predicted by the DFT calculations of Kresse et al. for the half-metal termination without the surface vanadyl species, is not consistent with our experimental results. We may therefore conclude either that the surface is vanadyl-terminated, or that this calculation yields an unphysical result not found in the total-energy cluster calculation of Czekaj et al.

The fact that the outermost V–O interlayer spacing is strongly contracted relative to the underlying bulk is also a feature of earlier structural studies of the (0001) surfaces of Al_2O_3 and Cr_2O_3 which also have the same bulk corundum structure. Both of these surfaces have also been found to be half-metal terminated, although in neither case was the possibility of O atoms in a vanadyl-like structure considered in their structural determinations. The LEED study of Al_2O_3 did consider the possibility of additional atop O atoms to simulate the possible effect of adsorbed water, but this model was not favoured in the analysis. Table 4 provides a comparison of the relaxation of the three outermost interlayer spacings found in these experimental investigations on Al_2O_3 and Cr_2O_3 and of our own study of V_2O_3. Evidently the large contraction of the outermost metal–oxygen interlayer spacing is a common feature of all the studies, with the value found for the V_2O_3 surface actually being the smallest value. Notice, though, that the SXRD study of Cr_2O_3 led to the conclusion that the best-fit structure was not a simple well-ordered relaxed half-metal termination, but rather one in which 1/3 of the surface Cr atoms were repositioned in interstitial sites – for this model the surface relaxations (the bracketed values in Table 4) were much smaller.

Of course, in the absence of lateral movements of the atoms within the layers, the large relaxations in the interlayer spacings in all of these surfaces would lead to large changes in the metal–oxygen nearest-neighbour bondlengths. In the case of the SXRD study of $Al_2O_3(0001)$ the possibility of lateral movements in the outmost O layer atoms was investigated to explore this possibility, and it was found that the best fit corresponded to radial movements of these O atoms away from the location of the adjacent Al atom in order to keep the local Al–O distance constant [19]. By contrast, in the LEED investigation of the $Cr_2O_3(0001)$ surface, no evidence for significant radial movements of the O atoms parallel to the surface was found [21]. To explore this possibility for $V_2O_3(0001)$ additional calculations were performed for the half-metal termination, starting from the best-fit structure as detailed in Table 2, in which this lateral expansion was explored together with re-optimisation of the outermost interlayer spacings. This yielded a structure with a slightly lower global *R*-factor (0.44 rather than 0.46) in which a lateral expansion of 0.10 Å was found with essentially no change (~0.01 Å) in the interlayer spacings. Evidently the small change in *R*-factor implies very poor precision, but formally this result indicates that the outermost V–O nearest-neighbour bondlength

Table 4
Comparison of the outermost layer relaxations, expressed as percentage changes from the bulk values, found in structure determinations of corundum-structure (0001) surfaces

Surface → parameter	$Al_2O_3(0001)$		$Cr_2O_3(0001)$		$V_2O_3(0001)$
	LEED [20]	SXRD [19]	LEED [21]	SXRD [22]	This study
O_{top}–M_{top}	−51%	−51%	−60%	−52% (−6%)	−31%
M'_{top}–O_{top}	+5%	+16%	−3%	−20% (0%)	−5%
M_2–M'_{top}	–	−28%	−21%	+18% (−26%)	−3%

M represents the metal (Al, Cr or V). In the case of the XSRD study of Cr_2O_3 the bracketed values correspond to a model in which 1/3 of the surface Cr atoms are in interstitial sites. For the present study the values given correspond to the ···V′OV (non-vanadyl) termination model with the lowest *R*-factors.

contraction associated with the outer layer relaxation is somewhat offset; compared with the bulk value of 1.96 Å, the surface value is 1.92 Å rather than the smaller value of 1.82 Å that would occur in the absence of this lateral relaxation.

An interesting issue raised by the two LEED studies is the vibrational amplitudes used in the analysis. In the case of $Al_2O_3(0001)$, a much improved fit was achieved by effectively using greatly enhanced vibrational amplitudes of the surface layer Al atoms perpendicular to the surface. In the LEED study of $Cr_2O_3(0001)$ the structural results were found to be sensitive to the choice of vibrational amplitudes of the O atoms; using a 'erroneously low' value of the Debye temperature for the O atoms in the original analysis actually led to very significantly different interlayer relaxations of (starting from the outermost value) −38%, −21% and −25% compared with the values in the final optimisation reported in their erratum of −60%, −3% and −21%. As these authors remark, the sensitivity of the structural parameter values to this vibrational parameter is unusual. In the analysis of the $V_2O_3(0001)$ surface reported here the vibrational amplitudes of the atoms in the bulk of the crystal were fixed at mean-square values (0.070 $Å^2$ and 0.066 $Å^2$ for V and O atoms, respectively) estimated from publications on VO_2 [36], Al_2O_3 [37] and V_2O_3 [38,39] in the corundum phase as well as comparison with the values used in the earlier LEED study of Cr_2O_3. The fact that the theoretically-simulated PhD spectra have similar modulation amplitudes to those of the experimental spectra strongly indicates that the values used are approximately correct; while LEED studies based on the use of the Pendry *R*-factor (as used in both the Al_2O_3 and Cr_2O_3 investigations) do not require any matching of absolute amplitudes, the *R*-factor we use in PhD does, and the vibrational amplitudes of the emitter and scatterer atoms has a pronounced effect on the modulation amplitudes through a Debye-Waller-like factor. We also note that our data are not consistent with a very greatly enhanced vibrational amplitude of the surface layer metal atoms, as was suggested in the LEED analysis of the Al_2O_3 surface; this would strongly attenuate the modulation amplitude of the surface V layer emitters, thus leading to far more bulk-like V 2p PhD spectra – by contrast, we find the V 2p PhD spectrum at normal emission is strongly sensitive to the large surface relaxation, clearly indicating that there is a substantial surface component in this spectrum.

In summary, our PhD investigation of the structure of the $V_2O_3(0001)$ surface provides clear support for the strongly-relaxed half-metal termination favoured by theoretical calculations and experimental studies of the related $Al_2O_3(0001)$ and $Cr_2O_3(0001)$ surfaces. The best-fit structure does *not* include the expected vanadyl V=O capping of this outermost half-metal layer, but a structure with closely-similar interlayer relaxations that includes the surface vanadyl species has associated *R*-factors that lie within our estimate variance. We cannot, therefore, exclude this alternative, vanadyl-terminated, structure. In part this failure to distinguish these two models may be attributed to the small number of vanadyl O atoms in this termination, compared to the number of subsurface O emitter atoms that contribute to our measured O 1s PhD spectra. A second factor, however, is the large variance associated with the rather high minimum value of the global *R*-factor for the best-fit structure. This high *R*-factor value may be attributable to the weak PhD modulations seen in most of the measured spectra. We note, however, that the LEED studies of the $Al_2O_3(0001)$ and $Cr_2O_3(0001)$ surfaces also led to relatively high values of the Pendry *R*-factor for measurements from clean surfaces. This apparent generic problem may be related to the problems of high-quality surface preparation on these oxide surfaces. Of course, in this regard there is a fundamental difference between PhD on the one hand, and any conventional diffraction technique such as LEED on the other. PhD is a local method that provides an incoherent sum of structural information over the whole surface, including regions that lack long-range order. LEED, on the other hand, relies on long-range order and samples selectively those regions of the surface that show long-range order. If the surface is partially disordered one would then expect LEED to provide more reliable structural information on the ordered components. The fact that LEED studies of these related surfaces also have high associated *R*-factors, however, suggests that the source of the common problem may be different.

Acknowledgements

The authors acknowledge the financial support of the Deutsche Forschungsgemeinschaft through the Sonderforschungsbereich 546, and of the Physical Sciences and Engineering Research Council (UK), together with the

award of beamtime by the BESSY synchrotron radiation facility.

References

[1] B. Grzybowska-Świerkosz, F. Trifirò, J.C. Vedrine (Eds.), Vanadia catalysts for selective oxidation of hydrocarbons and their derivatives, Appl. Catal. 157 (1997) 1.
[2] D.B. McWhan, T.M. Rice, J.P. Remeika, Phys. Rev. Lett. 23 (1969) 1384.
[3] S. Surnev, M.G. Ramsey, F.P. Netzer, Prog. Surf. Sci. 73 (2003) 117.
[4] A.-C. Dupuis, M. Abu Haija, B. Richter, H. Kuhlenbeck, H.-J. Freund, Surf. Sci. 539 (2003) 99.
[5] H. Niehus, R.-P. Blum, D. Ahlbehrendt, Surf. Rev. Lett. 10 (2003) 353.
[6] F.P. Leisenberger, S. Surnev, L. Vitali, M.G. Ramsey, F.P. Netzer, J. Vac. Sci. Technol. A 17 (1999) 1743.
[7] S. Surnev, L. Vitali, M.G. Ramsey, F.P. Netzer, G. Kresse, J. Hafner, Phys. Rev. B 61 (2000) 13945.
[8] S. Surnev, G. Kresse, M.G. Ramsey, F.P. Netzer, Phys. Rev. Lett. 87 (2001) 86102.
[9] S. Surnev, G. Kresse, M. Sock, M.G. Ramsey, F.P. Netzer, Surf. Sci. 495 (2001) 91.
[10] C. Klein, G. Kresse, S. Surnev, F.P. Netzer, M. Schmid, P. Varga, Phys. Rev. B 68 (2003) 235416.
[11] J. Schoiswohl, M. Sock, S. Eck, S. Surnev, M.G. Ramsey, F.P. Netzer, Phys. Rev. B 69 (2004) 155403.
[12] J. Schoiswohl, M. Sock, S. Surnev, M.G. Ramsey, F.P. Netzer, G. Kresse, J.N. Andersen, Surf. Sci. 555 (2004) 101.
[13] F. Pfuner, J. Schoiswohl, M. Sock, S. Surnev, M.G. Ramsey, F.P. Netzer, J. Phys.: Condens. Matter 17 (2005) 4035.
[14] I. Czekaj, K. Hermann, M. Witko, Surf. Sci. 525 (2003) 33.
[15] I. Czekaj, K. Hermann, M. Witko, Surf. Sci. 525 (2003) 46.
[16] I. Czekaj, K. Hermann, M. Witko, Surf. Sci. 545 (2003) 85.
[17] G. Kresse, S. Surnev, J. Schoiswohl, F.P. Netzer, Surf. Sci. 555 (2004) 118.
[18] P.D. Dernier, J. Phys. Chem. Solids 31 (1970) 2569.
[19] P. Guénard, G. Renaud, A. Barbier, M. Gautier-Soyer, Surf. Rev. Lett. 5 (1998) 321.
[20] C.F. Walters, K.F. McCarty, E.A. Soares, M.A. Van Hove, Surf. Sci. 464 (2000) L732.
[21] F. Rohr, M. Bäumer, H.-J. Freund, J.A. Mejias, V. Staemmler, S. Müller, L. Hammer, K. Heinz, Surf. Sci. 372 (1997) L291, erratum, Surf. Sci. 389 (1997) 391.
[22] Th. Gloege, H.L. Meyerheim, W. Moritz, D. Wolf, Surf. Sci. 441 (1999) L917.
[23] J. Ahn, J.W. Rabalais, Surf. Sci. 388 (1997) 121.
[24] K. Wolter, unpublished results cited in Ref. [4].
[25] D.P. Woodruff, A.M. Bradshaw, Rep. Prog. Phys. 57 (1994) 1029.
[26] D.P. Woodruff, Surf. Sci. Rep. 62 (2007) 1.
[27] E.A. Kröger, D.I. Sayago, F. Allegretti, M.J. Knight, M. Polcik, W. Unterberger, T.J. Lerotholi, K.A. Hogan, C.L.A. Lamont, D.P. Woodruff, Phys. Rev. B 75 (2007) 195413.
[28] K.J.S. Sawhney, F. Senf, M. Scheer, F. Schäfers, J. Bahrdt, A. Gaupp, W. Gudat, Nucl. Instrum. Meth. A 390 (1997) 395.
[29] G.A. Sawatzky, D. Post, Phys. Rev. B 20 (1979) 1546.
[30] T. Yamaguchi, Y. Miwa, J. Phys. Soc. Jpn. 45 (1978) 200.
[31] V. Fritzsche, J. Phys.: Condens. Matter 2 (1990) 1413.
[32] V. Fritzsche, Surf. Sci. 265 (1992) 187.
[33] V. Fritzsche, Surf. Sci. 213 (1989) 648.
[34] J.B. Pendry, J. Phys.C: Solid State Phys. 13 (1980) 937.
[35] N.A. Booth, R. Davis, R. Toomes, D.P. Woodruff, C. Hirschmugl, K.-M. Schindler, O. Schaff, V. Fernandez, A. Theobald, Ph. Hofmann, R. Lindsay, T. Giessel, P. Baumgärtel, A.M. Bradshaw, Surf. Sci. 387 (1997) 152.
[36] D.B. McWhan, M. Marezio, J.P. Remeika, P.D. Dernier, Phys. Rev. B 10 (1974) 490.
[37] M. Lucht, M. Lerche, H.-C. Wille, Yu. V. Shvyd'ko, H.D. Rütter, E. Gerdau, P. Becker, J. Appl. Cryst. 36 (2003) 1075.
[38] H.V. Keer, D.L. Dickerson, H. Kuwamoto, H.L.C. Barros, J.M. Honig, J. Solid State Chem. 19 (1976) 95.
[39] P. Pfalzer, G. Obermeier, M. Klemm, S. Horn, M.L. denBoer, Phys. Rev. B 73 (2006) 144106.